The current status of orbital experiments for UHECR studies

M I Panasyuk[1,2], M Casolino[3,4], G K Garipov[1], T Ebisuzaki[3], P Gorodetzky[5], B A Khrenov[1], P A Klimov[1], V S Morozenko[1], N Sakaki[6], O A Saprykin[7], S A Sharakin[1], Y Takizawa[3], L G Tkachev[8], I V Yashin[1] and M Yu Zotov[1]

[1] D.V. Skobeltsyn Institute of Nuclear Physics, M.V. Lomonosov Moscow State University (SINP MSU), Moscow 119991, Russia
[2] Faculty of Physics, M.V. Lomonosov Moscow State University, Moscow 119991, Russia
[3] RIKEN, 2-1 Hirosawa, Wako, 351-0198 Japan
[4] Istituto Nazionale di Fisica Nucleare – Sezione di Roma Tor Vergata, Italy
[5] APC, Univ Paris Diderot, CNRS/IN2P3, CEA/Irfu, Obs de Paris, Sorbonne Paris Cité, France
[6] Karlsruhe Institute of Technology (KIT), 76021 Karlsruhe, Germany. Now at: Osaka City University, Japan
[7] Central Research Institute of Machine Building (TsNIIMash), Korolev 141070, Russia
[8] Joint Institute for Nuclear Research (JINR), Dubna 141980, Russia

E-mail: `panasyuk@sinp.msu.ru`

Abstract.
    Two types of orbital detectors of extreme energy cosmic rays are being developed nowadays: (i) TUS and KLYPVE with reflecting optical systems (mirrors) and (ii) JEM-EUSO with high-transmittance Fresnel lenses. They will cover much larger areas than existing ground-based arrays and almost uniformly monitor the celestial sphere. The TUS detector is the pioneering mission developed in SINP MSU in cooperation with several Russian and foreign institutions. It has relatively small field of view ($\pm 4.5^\circ$), which corresponds to a ground area of $6.4 \cdot 10^3$ km^2. The telescope consists of a Fresnel-type mirror-concentrator (~ 2 m^2) and a photo receiver (a matrix of 16×16 photomultiplier tubes). It is to be deployed on the Lomonosov satellite, and is currently at the final stage of preflight tests. Recently, SINP MSU began the KLYPVE project to be installed on board of the Russian segment of the ISS. The optical system of this detector contains a larger primary mirror (10 m^2), which allows decreasing the energy threshold. The total effective field of view will be at least $\pm 14^\circ$ to exceed the annual exposure of the existing ground-based experiments. Several configurations of the detector are being currently considered. Finally, JEM-EUSO is a wide field of view ($\pm 30^\circ$) detector. The optics is composed of two curved double-sided Fresnel lenses with 2.65 m external diameter, a precision diffractive middle lens and a pupil. The ultraviolet photons are focused onto the focal surface, which consists of nearly 5000 multi-anode photomultipliers. It is developed by a large international collaboration. All three orbital detectors have multi-purpose character due to continuous monitoring of various atmospheric phenomena. The present status of development of the TUS and KLYPVE missions is reported, and a brief comparison of the projects with JEM-EUSO is given.

1. Introduction

The nature and origin of extreme energy cosmic rays (EECRs, those with energies $\gtrsim 50$ EeV[1]) remains one of the greatest puzzles of modern astrophysics after more than 50 years since their first registration [1]. In this introduction, we will briefly review a number of important experimental results on the subject that were obtained in recent years. These include results on the energy spectrum, mass composition and anisotropy of ultra-high energy cosmic rays (UHECRs) obtained with the Pierre Auger Observatory (Auger for brevity), located in Argentina (South hemisphere); High Resolution Fly's Eye (HiRes) and the Telescope Array Project (TA), both located in Utah, USA (North hemisphere). Then we recall the main idea behind observation of EECRs from space and review three orbital projects aimed to become the next generation of EECR experiments that are currently under active development mostly focusing on TUS and KLYPVE, but also briefly discussing the JEM-EUSO mission. We aim to explain how these projects are able to open new possibilities to solve the EECR puzzle.

The most important result relates to the all-particle energy spectrum of UHECRs. It was found by HiRes [2, 3], Auger [4] and confirmed by TA [5] that the flux of cosmic rays is strongly suppressed at energies $\gtrsim 50$ EeV. A joint working group of the Pierre Auger, Telescope Array and Yakutsk Collaborations concluded that the energy spectra determined by Auger and TA are consistent in normalization and shape within systematic uncertainties after energy scaling factors are applied [6]: both spectra demonstrate an "ankle" at around 5 EeV and a cut-off at $\gtrsim 50$ EeV. It was found though that the cut-off takes place at lower energies in the spectrum by Auger and is steeper than the TA one.

The cut-off was found at the energy scale predicted by Greisen [7] and independently by Zatsepin and Kuz'min [8], who demonstrated that the flux of protons will be strongly suppressed at energies $\gtrsim 50$ EeV due to the photopion production on the cosmic microwave background radiation. Still, the discrepancy in the energy spectra obtained by Auger and TA does not allow concluding if the observed cut-off is due to the GZK effect, due to the maximum energy attained in accelerators of EECRs, or a combination of both, see [9] for an in-depth discussion. It does not either allow one to make a definite conclusion concerning the mass composition of the primary particles: are they protons or heavier nuclei, e.g. iron.

Another discrepancy between results of the Auger and TA experiments further complicates the situation with the composition of UHECRs. Namely, the Auger data witness in favour of the mass composition becoming heavier at energies above 3 EeV [10] while the TA data are consistent with a light, dominantly protonic composition [11, 12] but incompatible with a pure iron composition. The TA results are also in agreement with previous HiRes stereo measurements. The elongation rate and mean values of the depth of the shower maximum measured at TA are in good agreement with Auger data [12]. Though one should keep in mind that, on the one hand, the measurement of masses of primary particles is one of the most difficult tasks in the physics of UHECRs since it is based on hadronic interaction models at energies far beyond the reach of man-made accelerators like the LHC. On the other hand, Auger and TA employ different analysis techniques and different cuts selecting data for the analysis, so that a direct comparison of the results of the two experiments can be misleading. A work on a detailed comparison of mass composition obtained with Auger and TA is in progress [13].

One more aspect of cosmic ray physics that attracts great attention is anisotropy of arrival directions of EECRs. It is one of the key elements in a search for possible sources but also useful for examining mass composition of EECRs independently of measurements of the shower depth. The most intriguing new result in the field is the discovery of a "hotspot" of cosmic rays with energies above 57 EeV made by the TA experiment in the Northern hemisphere [14]. The hotspot is a cluster of 19 (of 72 registered) events within a 20° radius circle centered at

---

[1] 1 EeV $= 10^{18}$ eV.

(equatorial coordinates) $(\alpha, \delta) = (146.°7, 43.°2)$ with an expected number of events equal to 4.49, which gives a (pre-trial) statistical significance of 5.1σ. The (post-trial) statistical significance of such a hotspot appearing by chance was estimated to be 3.4σ. The hotspot is located near the Supergalactic plane but there are no known specific sources behind it. It was suggested by the TA Collaboration that the hotspot may be associated with the closest galaxy groups and/or the galaxy filament connecting the Milky Way with the Virgo cluster; or, if EECRs are heavy nuclei in accordance with the Auger results, the hotspot events may originate in the Supergalactic plane and be deflected by the magnetic fields. Recently, it has been argued that the nearby starburst galaxy M82 and the bright nearby blazar Mrk 180 (or one of them) are likely sources of the TA hotspot assuming its events have a pure composition [15]. Still, the available statistics, the ambiguity in the mass measurements of EECRs and the insufficient knowledge of extragalactic magnetic fields do not allow making a definite conclusion.

The Pierre Auger Collaboration is also performing intensive studies of anisotropy. In particular, a correlation is reported between the arrival directions of cosmic rays with energies above 55 EeV and the distribution of active galactic nuclei (AGN) within 75 Mpc, among them the Centaurus A (Cen A) radiogalaxy, located at less than 4 Mpc distance [16, 17, 18]. More recently, Auger presented results of a whole number of tests aimed to search for signals of anisotropies of cosmic rays with energies above 40 EeV (with 231 of them having energies $\geq$ 52 EeV and zenith angles $< 80°$) [19]. None of the tests performed revealed a statistically significant deviation from isotropy but it was found that there is a certain excess of events with energies $\geq$ 58 EeV around the direction to Cen A and around AGN of the Swift catalogue within 130 Mpc and brighter than 10^{44} erg/s. In both cases, the probability of arising the excess by chance was estimated to be of the order of 1.3–1.4%. No hotspot similar to the one observed by TA was found. On the other hand, a similar study performed by TA using EECRs with energies $\geq$ 40 EeV registered by the surface detector during the first 40 months of its operation did not reveal any statistically significant correlations with AGN from a number of survey catalogues [20].

Another direction of anisotropy studies is a search for large-scale anisotropy of EECRs. Recently, Auger presented results of two Rayleigh analyses, one in the right ascension and one in the azimuth angle distributions, of the arrival directions of events with energy above 4 EeV with zenith angle up to $80°$ [21]. The largest departure from isotropy was found in the $E > 8$ EeV energy bin, with an amplitude for the first harmonic in right ascension $(4.4 \pm 1.0) \times 10^{-2}$, which has a chance probability of 6.4×10^{-5}. It was found that assuming the only significant contribution to large-scale anisotropy is from the dipolar component, the observations above 8 EeV correspond to a dipole of amplitude 0.073 ± 0.015 pointing to $(\alpha, \delta) = (95° \pm 13°, -39° \pm 13°)$, thus supporting an earlier result obtained for events with zenith angles $< 60°$ [22].

Telescope Array has also performed an analysis of large-scale anisotropy of cosmic rays at the highest end of the spectrum, though a totally different approach was employed [23]. Assuming pure proton composition, it was found that the distribution of events with energies > 10 EeV and > 40 EeV is compatible with the hypothesis of isotropy and incompatible with the distribution of local large-scale structure (LSS) at smearing angles smaller than $\sim 20°$ and $\sim 10°$ respectively. To the contrary, the data set composed of events with energy above 57 EeV was found to be compatible with the LSS model and incompatible with isotropy at (pre-trial) statistical significance $\sim 3\sigma$.

Anisotropy studies present a complicated task because none of the experiments observes the whole celestial sphere but a proper determination of the full set of multipole coefficients requires full-sky coverage. That is why a joint analysis of large-scale anisotropy of UHECRs with energies above 10 EeV performed by the TA and Pierre Auger collaborations is of special interest [24]. A declination band commonly covered by both experiments $(-15° < \delta < 25°)$ was used for

cross-calibrating the fluxes. The multipolar expansion of the UHECR flux obtained in the study allowed performing a series of anisotropy searches but no significant deviation from isotropy was revealed at any angular scale. It was later found that the obtained angular power spectrum contradicts the hypothesis that the distribution of UHECRs at energies above 10 EeV follows the LSS model if a purely protonic primary composition is assumed, in that amplitudes of low multipoles in the data are significantly lower than those calculated from the LSS model [25]. One of the possibilities to explain the result is that the primaries are heavy, as suggested by the Auger collaboration results.

Nowadays, obtaining definite conclusions concerning anisotropy of EECRs becomes one of the most important tasks. As is clear from the above, a considerable part of the difficulties in finding the sources of EECRs is due to (i) the limited statistics of events and (ii) the incomplete and non-uniform coverage of the celestial sphere by any of the modern experiments. Thus one needs to increase the statistics of EECRs providing a uniform exposition of the sky. This is exactly the field where orbital experiments open new horizons of research (not to mention a whole number of other scientific tasks related to astrophysics, fundamental physics and atmosphere sciences, which we do not discuss here) being complementary to ground-based detectors.

2. Observation of EECRs from space

The atmosphere of the Earth acts as a huge calorimeter for detecting UHECRs due to extensive air showers (EAS) produced by primary particles moving nearly at the speed of light. The secondaries of an EAS cascade ionize and excite molecules of nitrogen in the air, which then radiate photons in the range ≈ 330–400 nm. This near-ultraviolet (UV) air fluorescence light is produced isotropically and can be used to record the development of an EAS. The number of photons emitted at any point along the EAS track is proportional to the number of charged particles in the cascade, mostly electrons and positrons. Additional information can be obtained from the Cherenkov light diffusively reflected at the surface of the Earth. Both can be used to reconstruct the energy and arrival direction of the primary particle and to obtain information about its nature.

The idea of observing EECRs from space was put forward by Benson and Linsley more than thirty years ago [26].[2] They suggested to look earth-ward from a satellite flying on a circular equatorial orbit at height 500–600 km and equipped with a mirror 36 m in diameter with $10'$ resolution and ~ 5000 photomultiplier tubes 5 cm in diameter located at the focal surface of the mirror. They estimated that the instrument will have a circular field of view about 100 km in diameter (thus covering an area three times larger than that of Auger), a duty cycle of the order of 20–30%, and the energy threshold below 10 EeV.

While the basic idea might look simple, it was realized soon that such an experiment poses a whole number of challenging problems both in technology and science since one has to register a faint flux of photons emitted in the continuously varying conditions of the Earth atmosphere and background spoiled by man-made lights, star light and other phenomena with an instrument working in a harsh space environment and built with strong restrictions on mass, energy consumption, etc. Since the pioneering work by Benson and Linsley, different aspects of registering EECRs from space have been studied in great detail, see, e.g., [27, 28] and references therein. Still, not a single project of an orbital detector of EECRs has been implemented yet. In what follows, we will review the current status of development of the TUS and KLYPVE experiments and compare them with the most advanced of the existing projects, JEM-EUSO.

---

[2] One can find earlier dates in the literature but we failed to find a published work prior to this one.

3. TUS

The TUS (Tracking Ultraviolet Setup) experiment was started in 2001 [29] as a pathfinder for a more advanced KLYPVE project. Plans of accommodating the TUS detector on a satellite were changed several times and the detector itself was improved in comparison with the initial version [30, 31, 32]. Now it is accommodated on the Lomonosov satellite as a part of instrumentation for studying the Extreme Universe Phenomena [33] and is scheduled for launching in late 2015.

The TUS detector is based on the same optical scheme as the one suggested by Benson and Linsley but with a much more modest size of the elements. It consists of two main parts: a mirror-concentrator with an area of 2 m^2 and a photodetector composed of 256 pixels, located at the mirror focus, see figure 1. The technology of TUS was described elsewhere [34, 35, 36, 37] and only the main instrumental parameters are discussed below.


**Figure 1.** Detector TUS on board the Lomonosov satellite.

The mirror-concentrator is designed as an ensemble of 11 parabolic rings that focus a parallel beam to one focal point. In this design, the thickness of the mirror construction is small (3 cm) which is important for its deployment on the satellite frame. The focal distance of the mirror is 1.5 m. The mirror is cut into hexagonal segments with diagonal 63 cm. The segments are made of carbon plastic supported by a honey comb aluminum plate so that the whole construction is stable in a wide range of temperatures. The surface of the segments is obtained as plastic replicas of aluminum press forms (one for the central mirror part and one for 6 lateral parts). In a vacuum evaporation process, the plastic mirror surface is covered by aluminum film and protected by a MgF$_2$ coat. Reflectivity of the mirror surface at wavelength 350 nm (average for the atmosphere fluorescence) is 85%. The mirror passed various space qualification as well as optical tests. Those tests demonstrated sufficient stability of its optical quality in space conditions. Expected life time of the mirror is more than 3 years. The main parameters of the detector are listed in table 1. The mirror placed on the scientific payload frame of the Lomonosov satellite is shown in figure 2.

Optical tests were provided by two methods: 1) independent measurements of each mirror segment by scanning with parallel laser beams (described in detail in [38], 2) measurements with

a distant ($\sim$30 m) pinpoint light source. The first method allows one to evaluate the quality of production of the mirror segments surface. By the second method, final results on the point spread function (PSF) of the full size mirror at various beam angles were obtained. They are shown in figure 3.
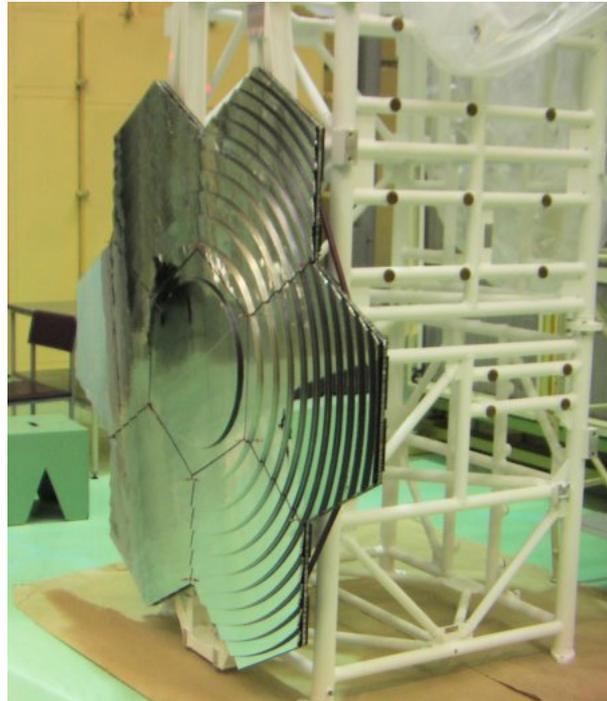
Figure 2. Mirror-concentrator of the TUS detector attached to the Lomonosov frame.
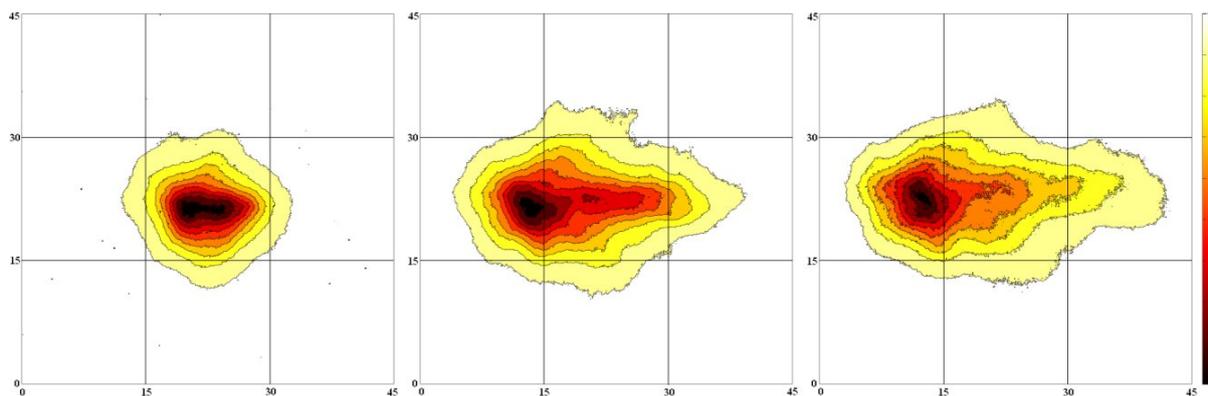
Figure 3. Results of the PSF measurement. Zenith angles from left to right: 0°, 3°, 4.5°. Dimensions are in millimeters. A square of 15×15 mm^2 corresponds to one pixel of the TUS photodetector.

The photodetector pixels are made by photomultiplier tubes (PMTs) R1463 of Hamamatsu with multi-alcali cathode of 13 mm diameter. The quantum efficiency of the PMT cathode is 20% for wavelength 350 nm. The PMTs multi-alcali cathode (instead of usually used bi-alcali one in ground-based fluorescence detectors) was chosen because the cathode operates in a wider

Table 1. Parameters of the TUS detector

Parameter, units	Value
Area of the mirror-concentrator, m^2	2
Mirror focal distance, cm	150
Pixel size, mm	15
Pixel number	256
Time step, μs	0.8
Observable area of the atmosphere at orbit height 500 km, km^2	6400
Pixel size in the atmosphere, km	5

range of temperatures in the linear regime. Light guides with a square entrance (15×15 mm) and circle output adjusted to PMT cathodes were used for making the detector field of view uniformly filled with pixels.

After preliminary testing, PMTs with a similar gain were grouped in 16 clusters. Data from each tube in a cluster are digitized by an analog-digital converter and then analyzed and memorized by a field-programmable gate array (FPGA). The final detector triggering and memorizing of all data is done by the central FPGA. Information volume of one EAS data is $\sim$100 Kbytes. Expected volume of one day EAS data transmitted to the mission center is 250 Mbytes. It is worth noticing that electronics of TUS is developed to measure not only EAS but also other transient phenomena in the atmosphere (lightnings, transient luminous events, meteors). This is achieved by recording waveforms of events with various time of digital integration (from 0.8 μs up to 6.6 ms). The duration of measured events varies from 205 μs up to 1.7 s. The TUS photodetector and one PMT cluster can be seen in figure 4.
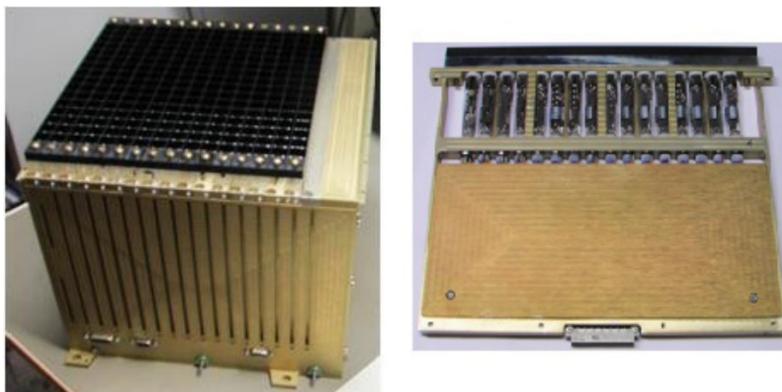
Figure 4. The TUS photodetector (left) and one PMT cluster (right).

Performance of the TUS detector was simulated taking into account parameters of the real TUS mirror-concentrator and TUS electronics [39]. The EECR trigger operates in two levels: at the first level, pixels with signals Z times larger than noise RMS are selected. At the second level, signals triggered on the first level and lined up in space in T consecutive time intervals are selected. Data from all pixels are recorded by a command of the second level trigger. Numbers Z and T will be set from the mission center for the optimal relation between the lowest TUS detector energy threshold and the trigger rate, limited by volume of information to be transmitted to the mission center.

Experimental results on the atmosphere glow were obtained during the Universitetsky-Tatiana-2 mission (Tatiana-2) [40]. The glow varies with the Moon phase and its height above the horizon but the atmosphere emits a glow even at moonless nights. Data of the Tatiana-2 mission, which include approximately $1.9 \cdot 10^4$ minutes of operation in night time, are presented in figure 5 as the operation time versus measured UV background intensity J. The background intensity varies from lower values at moonless nights (at the darkest atmosphere regions: above the Pacific ocean, above deserts and a part of Siberia) with $J = 3 \cdot 10^7$–10^8 ph cm^{-2} s^{-1} sr^{-1} to full-moon nights with $J \sim 3 \cdot 10^9$ ph cm^{-2} s^{-1} sr^{-1}.
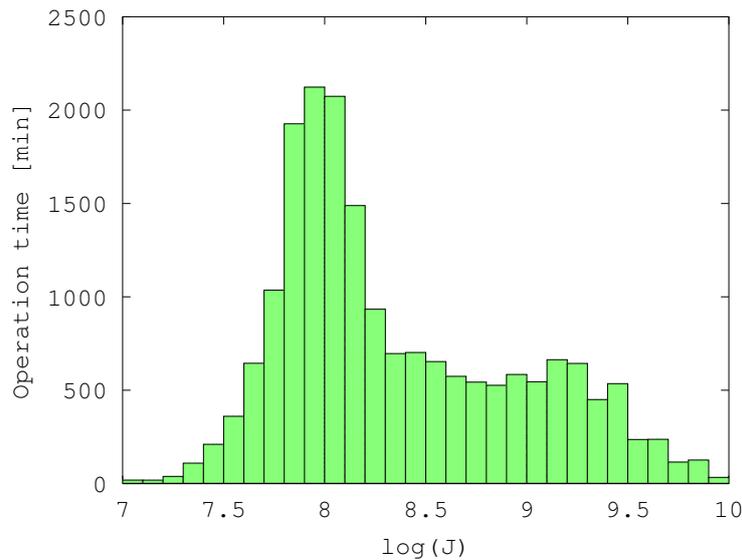

Figure 5. Operation time of Tatiana-2 as a function of the measured atmospheric background intensity J.

The Lomonosov satellite will be launched to a polar orbit close to that of Tatiana-2, so the available data can be used for estimating the TUS operation time with various background intensities. Results of such an estimate are presented in table 2. The number of registered EECRs will be much lower than those given in the table because the efficiency of the triggering system was not taken into account. With the limited exposure, the TUS detector will not make a breakthrough to the problem of EECR origin. Its main aim is to check the EAS fluorescence detector performance in a harsh space environment.

Table 2. Expected TUS performance parameters.

Intensity J, ph cm^{-2} s^{-1} sr^{-1}	$3 \cdot 10^7$–10^8	10^8–$5 \cdot 10^8$	$5 \cdot 10^8$–$5 \cdot 10^9$
One year night time (2047 hrs) vs J, %	33	39	28
TUS one year exposure, km^2 year sr	$3 \cdot 10^3$	$3.7 \cdot 10^3$	$2.7 \cdot 10^3$
Energy threshold (preliminary), EeV	60	150	400
EECR rate, events/km^2 year sr	0.024	0.002	0.0001
EECR event number per year	~ 70	~ 7	< 1

An important source of background events in orbital EECR measurements are UV flashes (duration of 1–100 ms), whose origins are related to electrical discharges in the atmosphere.
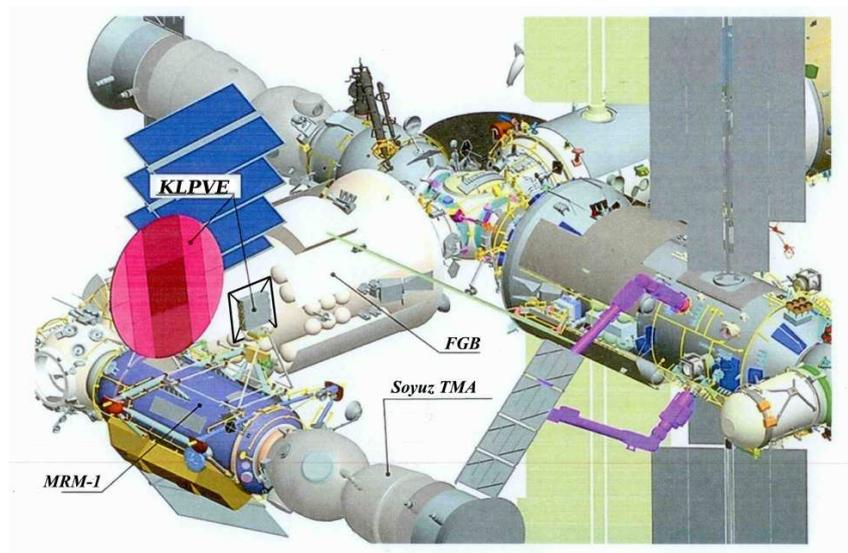
Figure 6. The KLYPVE detector on the MRM-1 module of the ISS.

In this respect, the data on UV flashes from the Tatiana-2 satellite were analyzed [41]. Measurements were done in a wide range of photon number Q in the atmospheric UV flashes: from $Q = 10^{21}$ up to $Q \sim 10^{25}$ where tens of events were registered. The main features of flashes with $Q > 10^{23}$, i.e., their duration of 10–100 ms and their global distribution concentrated in equatorial region above continents, allowed suggesting that those flashes are either lightnings or transient luminous events generically related to lightnings. Those "bright" flashes will be easily separated from EAS fluorescent signals due to their long duration and an enormous number of photons (to compare with EAS parameters: their duration is not more than 0.1 ms and the number of UV photons $Q \sim 10^{16}$ for $E = 100$ EeV).

More dangerous for imitation of EECR events is the background of dim and short flashes ($Q \sim 10^{21} - 10^{23}$, duration $\sim$1 ms) also observed by the Tatiana-2 detector. In contrast to bright flashes, dim ones are distributed more uniformly over the Earth. Rates of both kinds of flashes (about 10^{-4}–10^{-3} km^{-2} hr^{-1}) are much higher than the expected rate of EECR events $\sim 10^{-6}$ km^{-2} hr^{-1}, so that the problem of distinguishing EAS flashes from atmospheric flashes is a complicated one. In this respect, the performance of the TUS detector will be an important test of future space measurements of EECRs.

4. KLYPVE
In 2012, Skobeltsyn Institute of Nuclear Physics of Moscow State University finished the preliminary design stage of the KLYPVE[3] reflector type telescope for EECR measurements from the ISS. It will be located on the outer side of the Russian segment, see figure 6. The main component of the detector is a segmented optical system (OS) with a large entrance pupil. All parts of the telescope are to be delivered to the ISS by the Progress-TM vehicle.

The main goal of KLYPVE is to considerably increase the field of view (FOV) of the detector in comparison with TUS and to decrease the energy threshold. The mirror-concentrator has a reflective surface of about 10 m^2 (entrance pupil diameter 3.6 m, see figure 7). The OS has a focal distance of 3 m and FOV diameter of 15°. The angular resolution of the OS is the same as in the TUS detector, i.e., 5 mrad (pixel size 15 mm $\times$ 15 mm).

---

[3] KLYPVE is a Russian acronym for extreme energy cosmic rays.
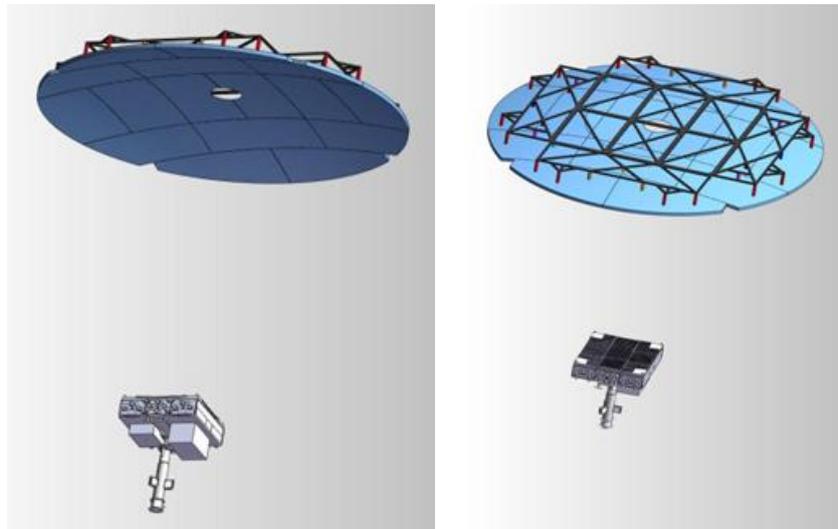
Figure 7. KLYPVE segmented mirror-concentrator and photodetector. Left: view from the front side, right: view from the rear side. A supporting frame is shown at the rear side of the mirror.

However, it became clear during the preliminary design phase that the characteristics of the instrument (observation area and image quality) do not allow solving the problems related to anisotropy of EECRs. The main reason for that is that due to the off-axis aberration of a fast optical system, the spot size increases very rapidly with increasing field angle. For an accurate reconstruction of EECR parameters (primary energy and direction), it is desirable to make a pixel of the photodetector smaller. Thus one has to look for optics with a much smaller spot size. These considerations initiated the development of a new OS for the KLYPVE detector in order to increase the FOV and to improve the spatial and angular resolution and the overall performance of the instrument. This work began in a close collaboration with members of the JEM-EUSO Collaboration in late 2013.

To eliminate the off-axis aberration, an additional corrective element was introduced into the telescope system in form of a Fresnel lens. The thickness of the lens should be sufficiently small, 1 cm in this case. The material of the lens is PMMA-000 (by Mitsubishi Rayon Co., Ltd.), which is a UV-transparent version of polymethyl metacrylate. It has a good UV transmittance (more than 90% for 15 mm thickness layer at wavelength more than 320 nm), with a refractive index of about 1.51 and has been used in space on many occasions. The lens has a radial Fresnel structure with groove depth 1 mm. Lenses with similar characteristics were manufactured at Ohmori Materials Fabrication Laboratory, RIKEN (Japan) in 2009–2011 [42].

Depending on the size and complexity of the forms of individual optical elements of the system, two approaches have been proposed.

4.1. Baseline System
In the so called Baseline system, the diameter of the reflector and the lens-corrector equals 3.4 m and 1.7 m respectively. The total length of the system (more precisely, the axial distance from the pole to the center of the focal surface) is equal to 4 m, the distance from the lens to the focal surface equals 70 cm, see figure 8. In this case, it is possible to expand the FOV up to $\pm 14°$, and the diameter of the image is not larger than 6 mm in the entire FOV. The angular resolution of the system is $\approx 0.057°$, which is equivalent to ~ 0.4 km at ground.
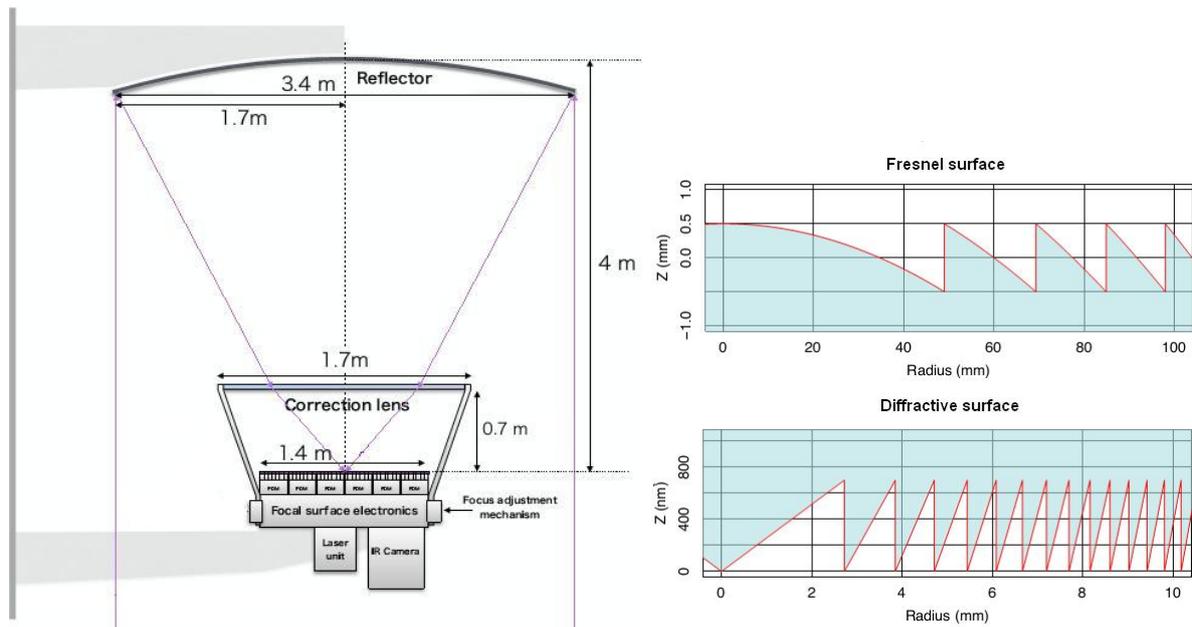
Figure 8. The optics of the Baseline system. Right: grooves of the Fresnel and diffractive structures of the corrective lens.

Table 3. Baseline OS performance characteristics for different field angles.

| Field Angle	0°	4°	6°	8°	10°	12°	13°	14°
Spot Size, mm	2.8	2.6	3.2	4.2	4.5	4.3	4.0	3.9
Optical Efficiency, %	62.8	61.7	58.8	57.4	51.4	43.8	37.1	29.6

One disadvantage of this approach is the difficulty of manufacturing of optical elements, especially lenses. To correct aberrations, both lens surfaces should have a small curvature, wherein the front side is a Fresnel spherical surface (with a radial structure of grooves of 1 mm depth), and the back side is a spherical diffraction surface (with grooves depth 700 nm, see the right side of figure 8).

Two main optical performance characteristics are the spot size and optical efficiency, which can be determined by non-sequential ray tracing. Table 3 represents these parameters for different field angles as RMS diameter of the focal surface image and as the ratio of the number of rays in the spot to the number of rays at the entrance pupil.

Delivering such a huge system to the ISS is a complicated task by itself. In case Progress-TM is used, cargo must be first placed inside the ISS and thus pieces of the instrument have to pass through a cylindrical lock of 70 cm diameter and 120 cm length. The currently offered solutions require segmentation of all the major components of the system, including the lens, the mirror and the photodetector, and subsequent deployment in space.

4.2. Multi-Eye Telescope System

The optical system of the KLYPVE is a wide-field large aperture and fast optics system. For such a complex instrument, a more promising option might be a Multi-Eye Telescope System
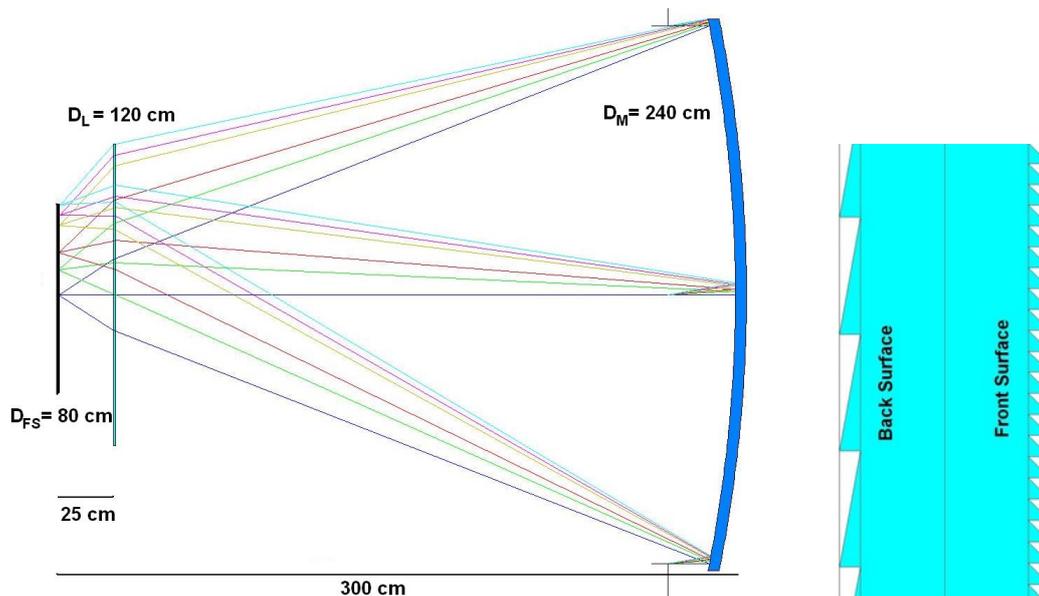
Figure 9. Left: the METS optical scheme. Right: grooves of the Fresnel structures at the edge of the corrective lens.

(METS). The main idea of METS is to divide a wide FOV into several FOVs of identical smaller telescopes. In this case, we have a simplification of an individual telescope: the design is simplified by cutting the aperture and the FOV of an individual telescope compared to the Baseline option thus reducing the requirements for their manufacturing.

This system has several additional advantages:

- smaller dimensions of individual telescopes and their narrower FOVs allow correcting aberrations without the use of a complex surfaces corrector (diffraction, curved Fresnel);

- not only manufacturing of the mirror segments and lenses but testing and adjustment of the overall system might be simpler;

- dimensions of the elements can be chosen basing on the possibility of transporting the individual telescopes assembled.

One of the possible drawbacks of METS is the necessity of a trigger working for all three telescopes simultaneously.

In the optimization calculations, the following dimensions of an individual telescope were obtained: 2.4 m diameter mirror, 1.2 m lens, 0.9 m photodetector, the total axial length 3 m, see figure 9. Correction of aberrations in the FOV $\pm 10°$ (which corresponds to the diameter of overall FOV of three telescopes $\sim 35°$) can be achieved using plane Fresnel surfaces. The angular resolution of METS is $\approx 0.075°$, which is equivalent to ~ 0.5 km at ground.

Spot size and optical efficiency of the METS telescope is presented in table 4. The sharp increase of the spot size on the edge of the FOV is due to the fact that a flat focal surface was used in the calculations.

To control spots within 5 mm, one should slightly bend the focal surface at the edges. Another advantage of the multi-eye system is the ability to use an active (dynamic) configuration. A special support structure of three telescopes can afford one to implement operation of the detector in various modes. In the basic mode, shown in the top row of figure 10, the FOVs of individual telescopes are adjacent (or slightly overlapping for cross-calibration). In the coincidence mode (overlapping FOVs), one can significantly reduce the energy threshold. Finally,
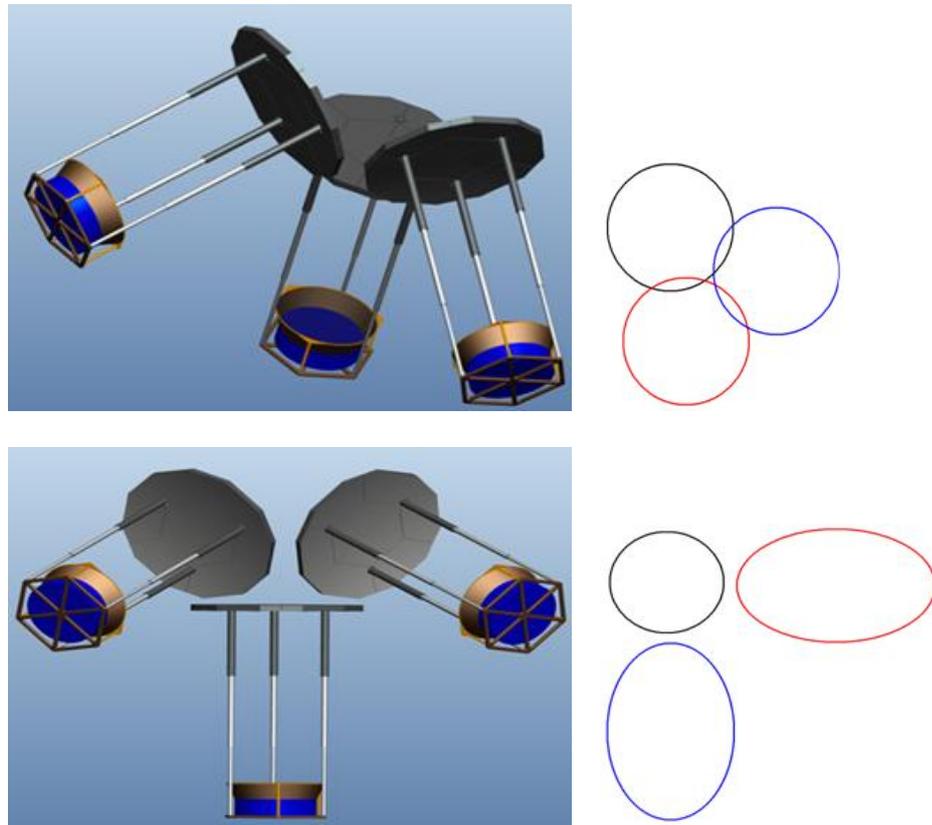
Figure 10. Top: the basic mode of METS operation. The angles of inclination of individual telescopes are exaggerated for clarity. Bottom: The tilted mode of METS operation. The right panels show mutual position of FOVs of separate telescopes.

Table 4. The METS OS performance characteristics for different field angles.

Field Angle	$0°$	$3°$	$5°$	$6°$	$7°$	$8°$	$9°$	$10°$
Spot Size, mm	2.0	2.7	3.7	3.7	4.0	4.2	4.5	5.4
Optical Efficiency, %	68.8	67.2	62.0	57.7	55.0	53.3	49.1	41.9

in the tilted mode (FOVs of two or all telescopes are inclined relative to the direction at the nadir, see the bottom row of figure 10), it is possible to increase the exposure, and hence to collect larger statistics of the EECR events.

5. JEM-EUSO

JEM-EUSO (the Extreme Universe Space Observatory on board the Japanese Experiment Module), which aims to be installed at the International Space Station (ISS), is the most ambitious and sophisticated of the three projects, see figure 11.

The instrument consists of a UV telescope and an atmospheric monitoring system. The telescope consists of three Fresnel lenses with an optical aperture of 4.5 m^2 and a focal surface detector formed by 137 photodetector modules composed of ~ 5000 multi-anode photo-multiplier tubes in total. The focal surface detector thus includes $\sim 3 \cdot 10^5$ channels providing a spatial
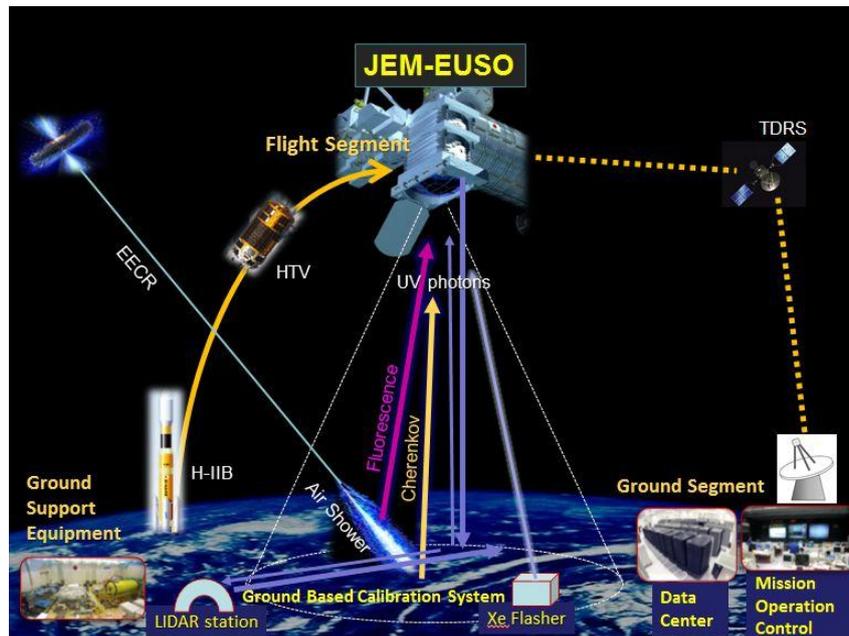
Figure 11. Principle of detecting EECRs with the JEM-EUSO telescope [43].

resolution $\approx 0.074°$, equivalent to ~ 0.5 km at ground. The opening angle of the telescope equals $60°$ providing an observational area of $\sim 1.4 \cdot 10^5$ km^2 in nadir mode. The annual exposure of JEM-EUSO for EECRs above 100 EeV is estimated to be an order of magnitude larger than that of Auger [44]. Thanks to the ISS orbit, JEM-EUSO is able to survey the entire celestial sphere almost uniformly, with the level of non-uniformity of the exposure on declination and right ascension $\sim 10\%$ [45]. Detailed simulations show that due to these factors JEM-EUSO will be able to detect significant anisotropies of EECRs practically in all feasible astrophysical scenarios [46] thus providing a huge step towards finding sources of EECRs. In December 2013, the Japanese Space Agency (JAXA) refused to deploy the instrument on board the JEM. A detailed discussion of the current status of the project and its pathfinders can be found in [47] and in dedicated contributions by A. Haungs and M. Fukushima in this volume.

6. Discussion

Figure 12 shows the dependence of the effective area S_{eff} of the Baseline and METS optical systems of the modified KLYPVE detector and the JEM-EUSO telescope on the field angle γ. Here, the effective area means the ratio of the luminous flux to irradiance, i.e.,

$$S_{\text{eff}} = \varepsilon_{\text{opt}}(\gamma) S_{\text{geom}}(0°) \cos \gamma,$$

where γ is the field angle, ε_{opt} is the optical efficiency, and the axial geometrical area (the second factor) takes into account the reduction of the entrance pupil due to the central screening by the lens. Thus, this parameter is one of the most important in the design of optical systems of an orbital detector.

The effective area is reduced at the edge of FOV for both systems, primarily due to an increase in the scattering on Fresnel and diffraction (in case of the Baseline system) grooves, which leads to a significant spot smearing at large field angles. As can be seen from figure 12, the effective area of the METS telescope approximately coincides with the JEM-EUSO one. In the case of the Baseline system, it is possible to increase the value of this parameter in average
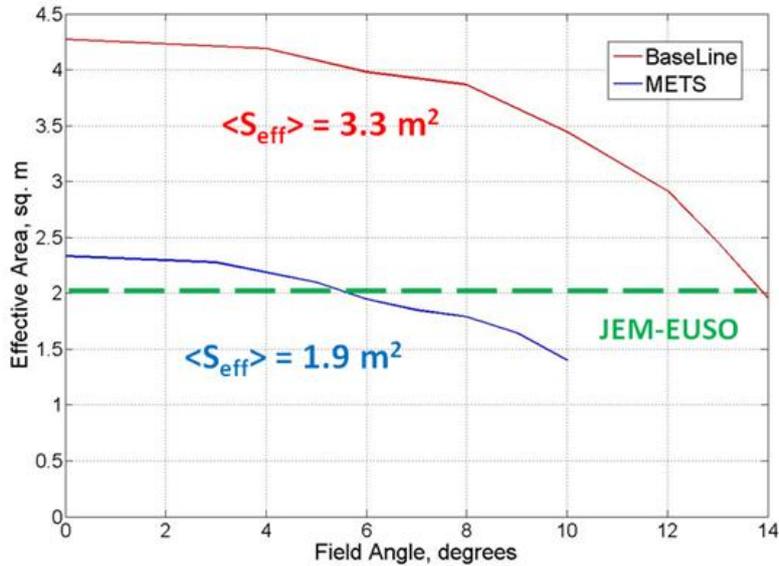
Figure 12. Effective area of the Baseline system and METS compared to JEM-EUSO for the entire FOV. $\langle S_{\text{eff}} \rangle$ denotes average values of the effective area for the isotropic distribution of light.

Table 5. Performance characteristics (spot size d, effective area S_{eff}, FOV Ω and throughput ΩS_{eff}) for 5 different orbital detectors of EECRs.

	d, mm	S_{eff}, m^2	Ω, sr	ΩS_{eff}, m^2 sr
JEM-EUSO	3	2	0.8	1.6
TUS	20	1.2	0.025	0.03
KLYPVE (orig.)	20	5	0.05	0.25
Baseline	3.5	3.5	0.2	0.7
METS	4	2.0	0.3	0.6

over the entire FOV by 70%, and more than twice for events in the cone $\gamma < 10°$. However, it should be noted that a refraction efficiency of the (first) diffraction peak was assumed to be 95% in these calculations. Reaching such values over the entire surface during manufacturing of the lens can pose a problem since the diffractive surface area is about 2.3 m^2. Thus, having undoubted advantages in decreasing the energy threshold, the Baseline system might have the effective FOV much smaller than the total FOV of the METS telescope.

Table 5 summarizes the main characteristics of the five optical systems: the lens system of JEM-EUSO, TUS Fresnel mirrors, the original version of the KLYPVE detector (without any corrector) and the two advanced options, the Baseline system and METS (with three identical telescopes in the basic mode of operation). Scattering of light by Fresnel surfaces was taken into account when calculating the effective area. It is important to underline that the effective area of the Baseline system provides an annual exposure two times larger than that of Auger, see figure 13. Together with an almost uniform exposure of both hemispheres, this gives an additional advantage for anisotropy studies.
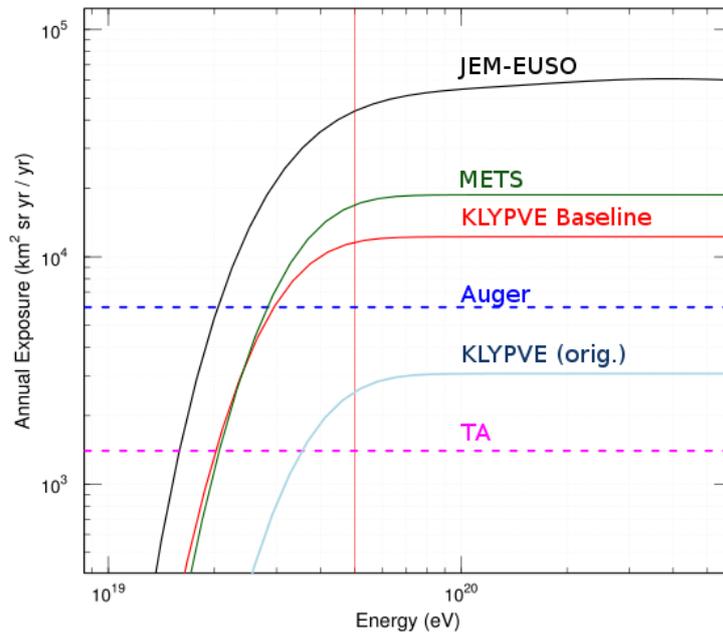
Figure 13. Annual exposure of different ground-based and space experiments.

7. Conclusions

Three orbital projects aimed at detecting extreme energy cosmic rays are being developed these days.[4] TUS is scheduled for launching in late 2015. If successful, TUS will become the pioneer of exploration of EECRs from space and a pathfinder for more advanced missions. It will also provide precious information about the UV background of the Earth atmosphere. The KLYPVE project finished the stage of the preliminary design and is included in the Russian Federal Space Program. It has entered the stage of the design project in its modified version aimed to improve the technical parameters of the instrument. There is a realistic possibility for KLYPVE to be installed on board the Russian Segment of the ISS in the next 6–7 years. The development of the full instrument of the JEM-EUSO project is currently facing certain problems, but the successful flight of EUSO-Balloon[5] on 24 August, 2014, which was used to test a number of components of the telescope and the atmospheric monitoring system, gives a strong ground for the hope that difficulties will be overcome and the most sophisticated of the three projects will be implemented in the future. Both KLYPVE and JEM-EUSO will provide outstanding possibilities for a breakthrough in solving the long-standing puzzle of the nature and origin of the most energetic particles ever detected on Earth.

---

[4] A discussion of the Super-$\mathcal{EUSO}$ [48] and OWL [49] missions goes beyond the scope of the article.

[5] See `http://euso-balloon.lal.in2p3.fr`

References

[1] Linsley J 1963 *Phys. Rev. Lett.* **10**(4) 146–48
[2] Bergman D R and High Resolution Fly's Eye Collaboration 2007 *Nucl. Phys. B Proc. Suppl.* **165** 19–26 (*Preprint* astro-ph/0609453)
[3] Abbasi R U *et al.* 2008 *Phys. Rev. Lett.* **100** 101101 (*Preprint* arXiv:astro-ph/0703099)
[4] Abraham J *et al.* 2008 *Phys. Rev. Lett.* **101** 061101 (*Preprint* arXiv:0806.4302)
[5] Abu-Zayyad T *et al.* 2013 *Astrophys. J. Lett.* **768** L1 (*Preprint* arXiv:1205.5067)
[6] Dawson B R, Mariş I C, Roth M, Salamida F, Abu-Zayyad T, Ikeda D, Ivanov D, Tsunesada Y, Pravdin M I and Sabourov A V 2013 The energy spectrum of cosmic rays at the highest energies *European Physical J. Web of Conf.* vol 53 p 1005 (*Preprint* arXiv:1306.6138)
[7] Greisen K 1966 *Phys. Rev. Lett.* **16**(17) 748–50
[8] Zatsepin G T and Kuz'min V A 1966 *Soviet J. of Experimental and Theoretical Physics Letters* **4** 78
[9] Harari D 2014 *Comptes Rendus Physique* **15** 376–83 (*Preprint* arXiv:1406.1117)
[10] Letessier-Selvon A 2014 *Brazilian J. of Physics* **44** 560–70 (*Preprint* arXiv:1310.4620)
[11] Tsunesada Y 2013 Study on mass composition of ultra-high energy cosmic rays by Telescope Array *Proc. 33rd Int. Cosmic Ray Conf. (Rio de Janeiro)*
[12] Abbasi R U *et al.* 2015 *Astropart. Phys.* **64** 49–62 (*Preprint* arXiv:1408.1726)
[13] Abu-Zayyad T *et al.* 2013 Pierre Auger Observatory and Telescope Array: Joint contributions to the 33rd Int. Cosmic Ray Conf. (ICRC 2013) (*Preprint* arXiv:1310.0647)
[14] Abbasi R U *et al.* 2014 *Astrophys. J. Lett.* **790** L21
[15] He H N, Kusenko A, Nagataki S, Yang R Z and Fan Y Z 2014 The possible extragalactic source of ultra-high-energy cosmic rays at the Telescope Array hotspot (*Preprint* arXiv:1411.5273)
[16] Pierre Auger Collaboration 2007 *Science* **318** 938–43 (*Preprint* arXiv:0711.2256)
[17] Pierre Auger Collaboration 2008 *Astropart. Phys.* **29** 188–204 (*Preprint* arXiv:0712.2843)
[18] Abreu P *et al.* 2010 *Astropart. Phys.* **34** 314–26 (*Preprint* arXiv:1009.1855)
[19] Pierre Auger Collaboration 2014 Searches for anisotropies in the arrival directions of the highest energy cosmic rays detected by the Pierre Auger Observatory (*Preprint* arXiv:1411.6111)
[20] Abu-Zayyad T *et al.* 2013 *Astrophys. J.* **777** 88 (*Preprint* arXiv:1306.5808)
[21] Pierre Auger Collaboration 2014 Large scale distribution of ultra high energy cosmic rays detected at the Pierre Auger Observatory with zenith angles up to 80° (*Preprint* arXiv:1411.6953)
[22] de Almeida R M 2013 Constraints on the origin of cosmic rays from large scale anisotropy searches in data of the Pierre Auger Observatory *Proc. 33rd Int. Cosmic Ray Conf. (Rio de Janeiro)* 0768 (*Preprint* arXiv:1307.5059)
[23] Fukushima M, Ivanov D, Kido E, Pshirkov M, Rubtsov G, Sagawa H, Thomson G, Tinyakov P, Tkachev I and Urban F 2013 Search for large-scale anisotropy of ultra-high energy cosmic rays with the Telescope Array *Proc. 33rd Int. Cosmic Ray Conf. (Rio de Janeiro)* 0935
[24] Aab A *et al.* 2014 *Astrophys. J.* **794** 172 (*Preprint* arXiv:1409.3128)
[25] Tinyakov P G and Urban F R 2014 Full sky harmonic analysis hints at large UHECR deflections (*Preprint* arXiv:1411.2486)
[26] Benson R and Linsley J 1981 Satellite observation of cosmic ray air showers *Proc. 17th Int. Cosmic Ray Conf. (Paris)* vol 8 pp 145–48
[27] Bugrov D *et al.* 2001 Modeling of space telescopes for observation of tracks produced in the Earth's atmosphere by extremely high energy cosmic rays *Mathematical modeling of complex information processing systems* ed Sadovnichii V and Doger Guerero E (Lomonosov Moscow State University Press) pp 98–118
[28] Pallavicini M, Pesce R, Petrolini A and Thea A 2012 *Astropart. Phys.* **35** 402–20 (*Preprint* arXiv:1105.2129)
[29] Khrenov B A *et al.* 2001 Space program KOSMOTEPETL (project KLYPVE and TUS) for the study of extremely high energy cosmic rays *Observing Ultrahigh Energy Cosmic Rays from Space and Earth* (*American Inst. of Physics Conf. Series* vol 566) ed Salazar H, Villasenor L and Zepeda A pp 57–75
[30] Khrenov B A *et al.* 2004 *Physics of Atomic Nuclei* **67** 2058–61
[31] Abrashkin V *et al.* 2006 *Adv. in Space Research* **37** 1876–83
[32] Abrashkin V *et al.* 2008 *Adv. in Space Research* **41** 2079–88
[33] Panasyuk M *et al.* 2012 *J. of Cosmology* **18** 7964–77
[34] Garipov G K *et al.* 2001 Electronics for the KLYPVE detector *Observing Ultrahigh Energy Cosmic Rays from Space and Earth* (*American Inst. of Physics Conf. Series* vol 566) ed Salazar H, Villasenor L and Zepeda A pp 76–90
[35] Tkachev L *et al.* 2009 *Nucl. Phys. B Proc. Suppl.* **196** 243–46
[36] Tkachenko A *et al.* 2011 Photo receiver of the orbital ultra high energy cosmic rays detector TUS *Proc. 32nd Int. Cosmic Ray Conf. (Beijing)* vol 11 p 272
[37] Tkachev L *et al.* 2011 The TUS Fresnel mirror production and optical parameters measurement. *Proc. 32nd*

Int. Cosmic Ray Conf. (Beijing) vol 3 p 124

[38] Grinyuk A, Slunecka M, Tkachenko A, Tkachev L, Klimov P and Sharakin S 2014 *Nucl. Inst. Methods in Phys. Res.* A **763** 604–609

[39] Khrenov B A *et al.* 2013 Pioneering space based detector for study of cosmic rays beyond GZK limit *European Physical J. Web of Conf.* vol 53 p 9006

[40] Vedenkin N N *et al.* 2011 *Soviet J. of Experimental and Theoretical Physics* **113** 781–90

[41] Garipov G K *et al.* 2013 *J. of Geophysical Research (Atmospheres)* **118** 370–79

[42] Hachisu Y *et al.* 2011 JEM-EUSO lens manufacturing *32nd International Cosmic Ray Conference (Beijing)* vol 3 p 184

[43] Ebisuzaki T, Medina-Tanco G and Santangelo A 2014 *Advances in Space Research* **53** 1499–1505

[44] Adams J H *et al.* 2013 *Astropart. Phys.* **44** 76–90 (*Preprint* `arXiv:1305.2478`)

[45] Bertaina M, Bobik P, Fenu F and Shinozaki K 2014 *Experimental Astronomy* URL `http://link.springer.com/article/10.1007%2Fs10686-014-9376-3`

[46] Rouillé d'Orfeuil B, Allard D, Lachaud C, Parizot E, Blaksley C and Nagataki S 2014 *Astron. & Astrophys.* **567** A81 (*Preprint* `arXiv:1401.1119`)

[47] Bertaina M and Parizot E for the JEM-EUSO Collaboration 2014 *Nucl. Phys. B Proc. Suppl.* B **256** 275–86

[48] Petrolini A 2011 *Nucl. Inst. Methods in Phys. Res.* A **630** 131–35 (*Preprint* `arXiv:0909.5220`)

[49] Krizmanic J F, Mitchell J W and Streitmatter R E 2013 Optimization of the Orbiting Wide-angle Light Collectors (OWL) mission for charged-particle and neutrino astronomy *Proc. 32nd Int. Cosmic Ray Conf. (Beijing)* ID 1085 (*Preprint* `arXiv:1307.3907`)